

Optimal pitwall profiles to maximise steepness in anisotropic bedded sedimentary rock

Andrea Agosti *OptimalSlope Ltd, London, UK*

Scott Cylwik *Call & Nicholas, Inc., Tucson, AZ, USA*

Stefano Utili *OptimalSlope Ltd, London, UK*

Abstract

Profitability and carbon footprint of an open pit mine depend to a large extent on the Overall Slope Angle (OSA) of its pitwalls. OptimalSlope, a new software for the design of slopes and pitwalls, determines geotechnically optimal non-linear profiles. Results obtained on four mine case studies in isotropic rock masses show optimal profiles can be up to 8 degrees steeper than their planar counterparts, i.e. fixed slope angle profiles exhibiting the same Factor of Safety.

OptimalSlope which has been recently modified to deal with anisotropic rock masses, is here employed to determine optimal profiles for an open pit mine to be excavated in a Cretaceous siltstone featured by 8 different joint sets and one main bedding. The recently introduced Cylwik's method was employed to establish direction dependent c and ϕ equivalent parameters from information on joint orientation and persistence for the relevant pit cross-sections. OptimalSlope simulations were run for several inclinations of the bedding dip (0, 15, 30, 45, 60, 75, 90) for three pitwall orientations (footwall, hanging wall, sidewall).

Measurements of the increase in OSA achieved by adoption of the optimal profiles over their planar counterparts are provided. Stability analyses by Rocscience Slide2 were also performed to independently verify the FoSs of the calculated optimal profiles.

1 Introduction

Pitwall inclinations bear a very significant effect on mine environmental impact and profitability since they control to a large extent the amount of rockwaste to be excavated (Hustrulid et al. 2013). Between 1930 and 2000, the depth of the average discovery in Australia, Canada, and the United States increased from surface outcropping to 295 m (Randolph 2011). Consequently, ensuring pitwalls as steep as possible has grown in importance and it will be even more so in the future.

Anecdotal evidence that slope profiles non-linear in cross-section, i.e. a profile whose inclination varies with depth, are better than linear ones was first reported as far back as 1890 (Newman 1890). Newman observed that cuttings of concave shape excavated in homogeneous clay layers tended to be more stable than planar ones with the same OSA, which are more stable than cuttings of convex shape. Almost a century later, Hoek & Bray, in chapter 12 of the second edition of Rock slope engineering (Hoek & Bray 1977), analysed the stability of some concave circular slopes in cross-section. They found the stability number, a dimensionless index capturing the mechanical stability of a slope introduced by Taylor (1937), for circular profiles to be higher than their planar counterparts, i.e. the planar slopes with the same OSA, which share the same toe and crest points. After that, the first systematic theoretical study on the mechanical properties of concave slope profiles for geomaterials exhibiting some cohesion, so applicable to all rocks and clayey soils, appeared in (Utili & Nova 2007). By employing the upper bound theorem of limit analysis, Utili & Nova proved that logspiral profiles exhibit higher FoS than their planar counterparts for any value of c and ϕ considered. Later, other researchers (Jeldes et al. 2015, Vahedifard et al. 2016, Vo & Russell 2017) have independently reached the same conclusion concerning the superior stability of concave profiles albeit employing different methods for assessing slope stability, e.g. the slip line method, limit equilibrium methods (LEM), and the finite element method. A fundamental limitation of the studies listed above is the assumption that the shape claimed to be optimal is found as the shape associated with the highest stability number among curves belonging to a very restricted family and the assumption of uniform slope. More recently, a new geotechnical software, OptimalSlope (Utili, 2016), has been introduced which calculates the slope optimal profile for any specified lithological sequence without unduly restricting the search to any predefined family of shapes. To be able to quantify the gains of Net Present Value (NPV) and carbon footprint reduction in a consistent way in (Utili et al. 2022) and (Agosti et al. 2021a, b) the open pit mines considered were designed twice employing the same pit optimiser software, economic parameters and optimisation strategy, with the only difference between the two designs being the pitwall profiles adopted. Financial and environmental gains were calculated as the difference between the NPV, carbon footprint and energy consumptions resulting from the two designs.

A fundamental limitation in the aforementioned works is the assumption of isotropic rock mass strength. However, accounting for the directional dependence of rock strength is increasingly a requirement of the open

pit mining industry as shown by the increasing numbers of publications dedicated to rock mass strength anisotropy in key geotechnical and mining conferences (e.g. Slope stability conference in 2013, Asia Pacific Slope Stability in mining conference in 2016, Slope Stability Symposium in 2018, 2020 Symposium on Slope stability in Open pit mining, Second International Slope Stability in Mining conference 2021), LOP guidelines (Read & Stacey 2009, Martin & Stacey 2018) and also driven by the availability of general anisotropic shear strength models in Rocscience Slide2 and RS2.

In this paper, the methodology presented in (Utili et al. 2022, Agosti et al. 2021a, b) for the design of geotechnically optimal pitwall profiles is extended to rock masses of anisotropic shear strength. A case study of a mine excavated in a typical bedded sedimentary rock mass is considered. The novel methodology recently introduced by Cylwik (2021) to determine equivalent anisotropic c , ϕ parameters for jointed rock mass is employed. The paper is structured as follows: in Section 2, the main modelling techniques in the literature for anisotropic shear strength of rock masses are reviewed and the model here adopted, i.e. directionally dependent equivalent c , ϕ parameters characterizing the shear strength of the jointed rock mass, is presented; in Section 3 the case study is introduced together with the determination of the anisotropic shear strength parameters; in Section 4 the extension of OptimalSlope to anisotropic rock masses is introduced; in Section 5 the optimal profiles determined by OptimalSlope are illustrated for several scenarios of pit excavation; in Section 6 conclusions are provided.

2 Modelling anisotropic rock mass shear strength

An equivalent continuum approach to model rock mass anisotropy, i.e. the use of equivalent shear strength parameters, is here employed. The Mohr-Coulomb (M-C) criterion was extended to account for anisotropic behaviour of soils since (Lo 1965). Important work has also been performed by (Chen 1975) employing the limit analysis upper bound method to investigate the stability of slopes in anisotropic soils with the strength parameters c and ϕ assumed to vary with the loading direction according to sine and cosine functions. This work was recently extended to account for tension cracks by (Stockton et al. 2019) using the LEM. However, it is now well established that the strength of rocks is better described by the H-B criterion rather than the M-C (Read & Stacey 2009) and the type of directional dependency exhibited by soil shear strength cannot be assumed for rock. However the H-B criterion (Hoek & Brown 1980) and its extension to rock masses, generalised H-B (G-H-B) (Hoek et al. 2002) were formulated for isotropic rocks. Although recently important work has been performed to extend the G-H-B to anisotropic intact rock (Colak & Unlu 2004, Saroglu and Tsiambaos 2007, Ismael et al. 2014), nevertheless the presence of discrete discontinuities such as bedding planes and joint sets are not currently captured by the aforementioned extensions of the G-H-B criterion.

To capture the effect of discontinuities on the rock mass strength, Ryan (2005) proposed a method to determine equivalent c , ϕ anisotropic parameters for a rock mass featured by a single joint-set in 2D with the resulting c , ϕ parameters varying non linearly with the direction of loading. Recently Cylwik has fundamentally extended the method that now allows estimating the equivalent c , ϕ parameters for rock-masses with any number of joint-sets in 3D accounting for information on both orientation and persistence of the joint-sets (Cylwik 2021). A worksheet (see Figure 3) estimates the strength for any directions of shear and for any cross-section orientation on the basis of intact rock strength, rock discontinuity set statistics, discontinuity strength, and RQD. The method provides reduced strength for shear in the directions parallel to jointing and increased strength for shear in directions non-parallel to jointing, with a continuous function of strength in between the two extremes. Details on the methodology can be found in Cylwik (2021) and are not repeated here. A key observation is that the anisotropic model resulting from the determination of the equivalent c , ϕ parameters can be highly non-linear with the anisotropic strength of the rock mass varying continuously with the direction of loading (see Figure 3). Therefore, it is important to input the c versus loading shear direction and ϕ versus loading shear direction functions correctly in any software employed for the analysis of slope stability.

3 Case study

The rock mass considered for this study is a Cretaceous-age siltstone located at a mine in central Mexico. The siltstone exhibits predominant bedding and cross-bedding, which is variable in orientation due to gentle undulating folds across the property. A photograph of the rock mass is shown in Figure 1.



Figure 1 Photograph of the siltstone of the mine case study considered.

3.1 Structural data

The cell mapping technique was used to collect joint set orientation, length, and spacing data (Nicholas & Sims 2000, Call 1992). A negative exponential distribution is used to model both joint spacing and length. To combine mapping cells from across the site, the structural data from each group of cells was rotated so that the mean vector of the bedding set is flat (dip and dip direction of zero degrees). The structural dataset, rotated so that the flat bedding orientation is at 0 degree, is shown in the lower hemisphere stereonet in Figure 2.

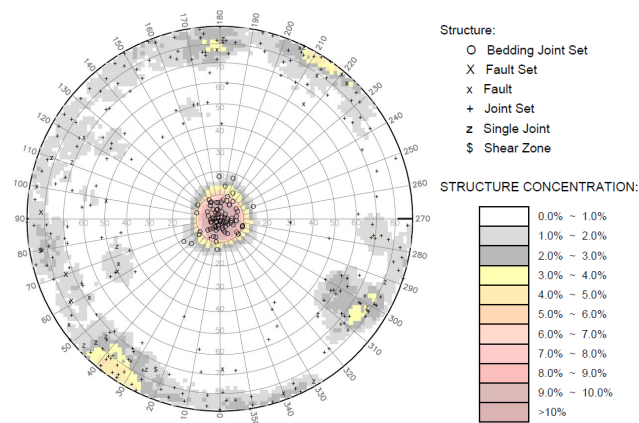


Figure 2 Lower hemisphere stereonet of siltstone structural data.

3.2 Rock strength testing

Direct shear tests were performed on natural fractures from core drilling in the siltstone to determine mean values of the joint friction angle and cohesion. These result in a mean friction angle of 24.2 degrees. Uniaxial and triaxial compression testing was performed on 25 HQ3-size intact core samples (63.5 mm diameter) and resulted in a mean intact internal rock friction angle of 48.6 degrees and cohesion of 8924 kPa. The measured density of the rock is 26.2 kN/m³.

3.3 Anisotropic strength estimation

The anisotropic strength of the bedded siltstone was estimated using the calculation worksheet downloaded from Cylwik (2022). Example input parameters and estimated anisotropic strengths are shown in Figure 3 for a bedding dip of 60 degrees. Lower hemisphere stereonets show both the structure data and estimated anisotropic strengths. Charts of rock mass cohesion and friction angle are shown for cross section azimuths of 0, 180, and 270 degrees. The azimuths of 0 and 180 degrees exhibit highly anisotropic behaviour versus dip angle, while the azimuth of 90/270 degrees shows relatively isotropic strength.

		Probability of Occurrence	Dip Direction (deg)	Dip (deg)	Mean Length (ft/m)	Mean Spacing (ft/m)	Strength Reduction Along Joints
Fracture Strength							
Cohesion	28 kPa						
Phi	24.2 deg						
Intact Rock Strength							
Cohesion	8,924 kPa						
Phi	48.6 deg						
RQD: 30%							

Joint Set 1	1.00	180	60	15.8	0.2	0.00
Joint Set 2	0.44	109	89	10.1	1.4	0.57
Joint Set 3	0.33	342	43	6.1	1.3	0.69
Joint Set 4	0.26	46	52	7.5	1.3	0.75
Joint Set 5	0.42	264	63	7.0	1.4	0.60
Joint Set 6	0.19	337	26	7.7	1.6	0.82
Joint Set 7	0.37	65	39	7.1	1.3	0.65

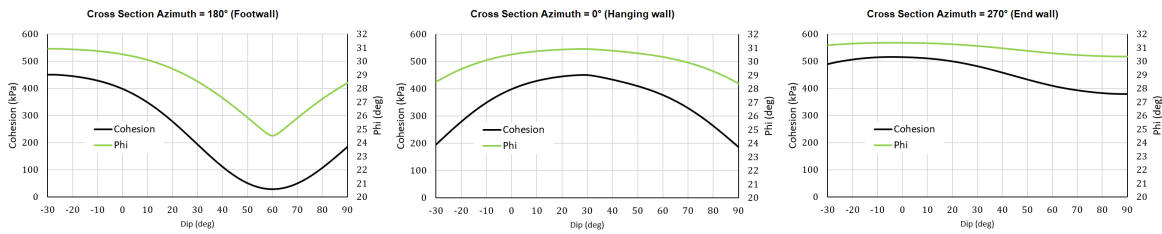
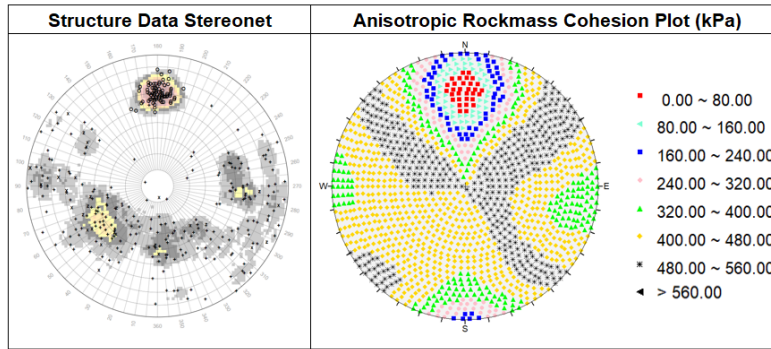


Figure 3 Calculation worksheet to calculate equivalent anisotropic, i.e. direction dependent, c and ϕ values versus the (apparent) dip angle of the shear plane for a bedding dip of 60 degrees to the south (after (Cylwik 2021)).

4 SENSITIVITY ANALYSIS

4.1 Joint dataset and 2D sections considered

To consider the effects of anisotropic rock mass strength on the geotechnically optimal slope profile, a sensitivity analysis was conducted considering different inclinations of bedding within the siltstone. Dip values of 0, 15, 30, 45, 60, 75, and 90 degrees for the bedding dipping to the south were analysed by rotating the structural data in three dimensions. Three different wall orientations in relation to the dip direction of bedding were analysed, for a total of 21 pitwall scenarios. The three different wall orientations considered are here termed as the footwall, hanging wall, and end wall according to classical open pit terminology. An example of the wall orientations in relation to bedding is shown on the stereonet in Figure 4. The mining nomenclature definitions for the highwall in relation to the dip direction of bedding are adopted for this paper, namely:

- On the Footwall bedding is dipping into the excavation. (DDR=180°)
- On the Hanging Wall bedding is dipping back into the slope. (DDR=0°)
- On the End Wall bedding is dipping perpendicular to the slope. (DDR=90° or 270°)

The siltstone rock mass utilized for this study is representative of many bedded ore deposits that contain well defined bedding and cross bedding discontinuity sets. The results of this sensitivity study are relevant for numerous mining environments throughout the world, as many economic deposits are strata-bound and therefore the slopes exhibit footwall/hanging wall geometries. The following parameters are considered in our analysis:

- 195-meter high slope with 15-meter benches
- Max inter-ramp slope angle of 55 degrees (controlled by bench geometry parameters)
- Design acceptance criterion of Factor of Safety ≥ 1.30 .

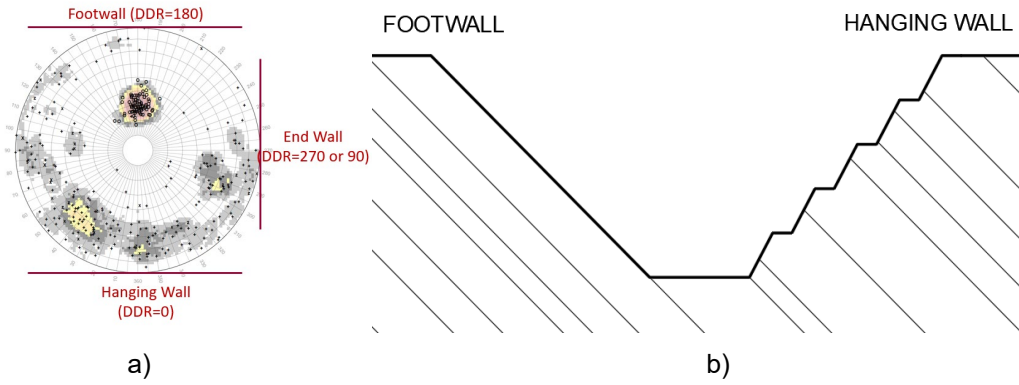


Figure 4 a) Example of Stereonet of bedding with footwall, hanging wall, and end wall orientations shown. b) Visualisation of footwall and hanging wall in the reference vertical cross section.

4.2 Pitwall design

As per standard mining practice benches are designed first and then the overall pitwall profiles (Read & Stacey 2009, Darling 2011). The height of the benches adopted for the whole mine is 15m. We computed the minimum berm width, b_w , using the equation proposed in Hartman et al. (1992) derived from the modified Ritchie's criteria, which has been demonstrated to be effective in field tests in several benched mine slopes (Ryan & Pryor 2001):

$$b_w[m] = 4.5[m] + 0.2 \cdot H_{bench} \quad [1]$$

The maximum bench face angle was assumed to equal to 70 degrees based on mining equipment specifications. We then verified the FoS (in this case $FoS \geq 1.0$) by the Limit Equilibrium Method Morgenstern-Price using the Rocscience program Slide2.

OptimalSlope requires bench height, bench face inclination, minimum berm width and road width as input from the user since these geometric data will act as constraints in the search for the optimal profile (Utili et al. 2022). Any pitwall profile is defined in OptimalSlope by a discrete set of points in the vertical plane: see the (x_i, z_i) coordinates in Figure 5, with z_i being values specified according to the bench height ($\Delta z = \text{bench height}$) input by the user whilst x_i are unknown variables to be determined. The search for the optimal profile is constrained to feasible profiles (which lie within the red and blue bounds of Figure 5). A profile is feasible if

$$\frac{z_i - z_{i-1}}{x_i - x_{i-1}} \leq \tan \alpha_{i \max} \quad [2]$$

for every i , i.e. the inclination of each segment of the profile is capped to $\alpha_{i \max}$. The $\alpha_{i \max}$ values are determined by the code before the optimization algorithm is called on the basis of bench height, bench face inclination and minimum berm width provided by the user (see Figure 5b). In case a ramp needs to be included as part of the pitwall profile, a lower $\alpha_{i \max}$ value is imposed for the profile segment corresponding to the vertical position of the ramp.

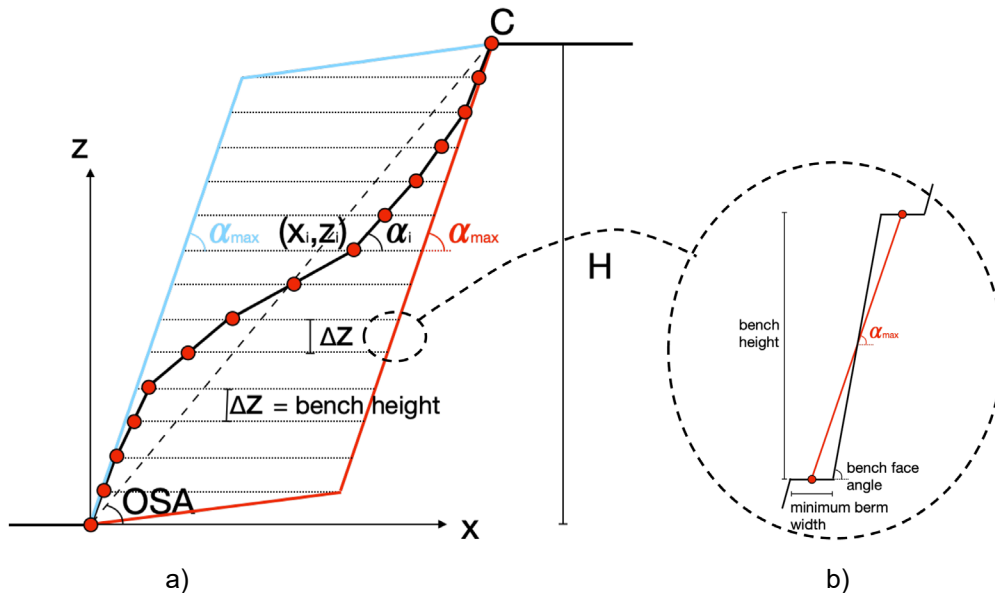


Figure 5 a) A generic candidate slope profile. The toe of the profile is at the axes origin (x_0, y_0) , point C is the slope crest. A uniform discretization along the z direction is adopted. The red and blue lines enclose the region where the profiles are sought. The profile is discretised in $n \Delta z$ intervals so there are $n-1$ unknowns to be determined: x_1, x_2, \dots, x_{n-1} with Δz equal to the bench height. b) determination of α_{max} based on bench geometry (after (Utili et al. 2022)).

The optimal pitwall profile is defined as the overall steepest safe profile, *i.e.* $OSA=OSA_{max}$, with OSA being the inclination over the horizontal of the line joining the pitwall toe to the crest (see Figure 5). OSA_{max} is determined by OptimalSlope iteratively. Firstly, an initial OSA is heuristically determined using a database of stability charts derived from (Hoek & Bray 1977) based on some equivalent geomaterial geotechnical properties and the specified FoS. Then, the main algorithm calculates the optimal pitwall shape for an assigned OSA and geometric constraints (bench height, bench face inclination, minimum berm width and road width). The FoSi associated with the optimal profile found at the i -th iteration is then compared to the target FoS_{target}: if it is higher, a steeper OSA is prescribed at the next iteration, vice versa if lower, a flatter OSA is prescribed. The termination criterion is specified in terms of the percentage difference between FoS_{target} and FoS_i.

5 Extension of OptimalSlope to anisotropic rock masses

For the purpose of this paper, we developed a new version of OptimalSlope (Utili 2016) capable of dealing with anisotropic rock masses. A complete and detailed explanation of how OptimalSlope works can be found in (Utili et al. 2022). Therefore, in this paper, we will only summarize the main concepts and mainly focus on introducing the implementation of the anisotropic strength criterion.

In the case of a homogeneous slope characterized by anisotropic rock strength, the optimal profile shape is found by the main algorithm, for a prescribed input OSA, as the profile associated with the largest stability factor, that is a dimensionless single scalar parameter which was initially introduced by (Taylor 1937) to develop dimensionless stability charts, and it is to date widely used to compare the performance of different slopes. For the case of an anisotropic M-C geomaterial, the general expression of the stability factor can be modified with:

$$N_s = \frac{\gamma H \cdot FoS}{c_{rm}} \quad [3]$$

with, γ the rock unit weight, H the slope height and c_{rm} the equivalent cohesion for the rock mass.

Within OptimalSlope's main algorithm (Figure 6), the stability factor is computed by using the upper bound theorem of limit analysis, which states that a slope will collapse under its own weight if, for any assumed kinematically admissible failure mechanism, the rate of external work done by the soil weight exceeds the rate of internal energy dissipation (Chen 1975). In the framework of limit analysis, only Chen (1975) approached the problem of an anisotropic slope. However, to not violate the kinematical admissibility, he assumed that only the cohesion parameter was anisotropic, *i.e.* the angle of internal friction was assumed to remain isotropic throughout the calculations. Neglecting the anisotropy of the internal friction angle may indeed affect the depth and position of the critical failure surface found by LE and FEM analyses. Moreover, the transversally isotropic model employed by Chen (1975) was proven to return unrealistically low FoS due to the conservative strength transition between rock mass and bedding (Mercer, 2012). Instead OptimalSlope's new anisotropic strength criterion builds on the equations developed by Chen (1975) by computing, for any assumed failure mechanism, the expressions of the external and dissipated work heuristically. First, for any assumed failure mechanism (Figure 6a), the failure surface is subdivided into piecewise segments. Then, the code computes, for each piecewise segment, the average inclination ($\alpha_{fail,i}$) which is used, in conjunction with the relationships between c , φ and the apparent dip of the failure surface from Section 2, to calculate the differential shear strength and the corresponding values of c and φ (Figure 6b) which are used in the expression of the rate of dissipated energy and rate of external work. The c versus loading shear direction and φ versus loading shear direction functions are provided in discretised form as a series of points. To obtain a result independent on the choice of discretisation, a discretisation interval no larger than 1 degree was employed.

The stability factor (N_s) for the assumed failure mechanism can be computed equating the rate of dissipated energy and the rate of external work. Finally, with a proprietary optimization algorithm, OptimalSlope will iterate through all the possible failure mechanisms and slope profile shapes to converge to the profile associated with the largest stability factor, *i.e.* the optimal profile.

Note that the methodology proposed is valid for any anisotropy function. The normal stress – shear strength functions here employed are linear. However, in case of non-linear functions, *e.g.* Barton-Bandis for the bedding strength, they could also be implemented once linearized by a sufficiently small discretization.

Figure 7 Sensitivity analysis on tension crack depth. a) The most critical tension crack depth corresponds to an FoS lower than the FoS_{target} , the OSA will be reduced, and the most critical tension crack will be reevaluated. b) A tension crack on the slope profile.

5.2 Determination of optimal profiles

We computed the geotechnically optimal slope profiles for the 3 different cross sections established for the mine (see Section 6). OptimalSlope runs on the AWS Batch cloud (AWS 2022). The software architecture is summarized in Figure 8: the input data needed for each pitwall to be designed are received from the OptimalSlope local client application, then a dedicated AWS EC2 instance is created and run for each job submitted. Finally, upon the termination of the simulation, the results are returned to the OptimalSlope local client application for visualisation by the user.

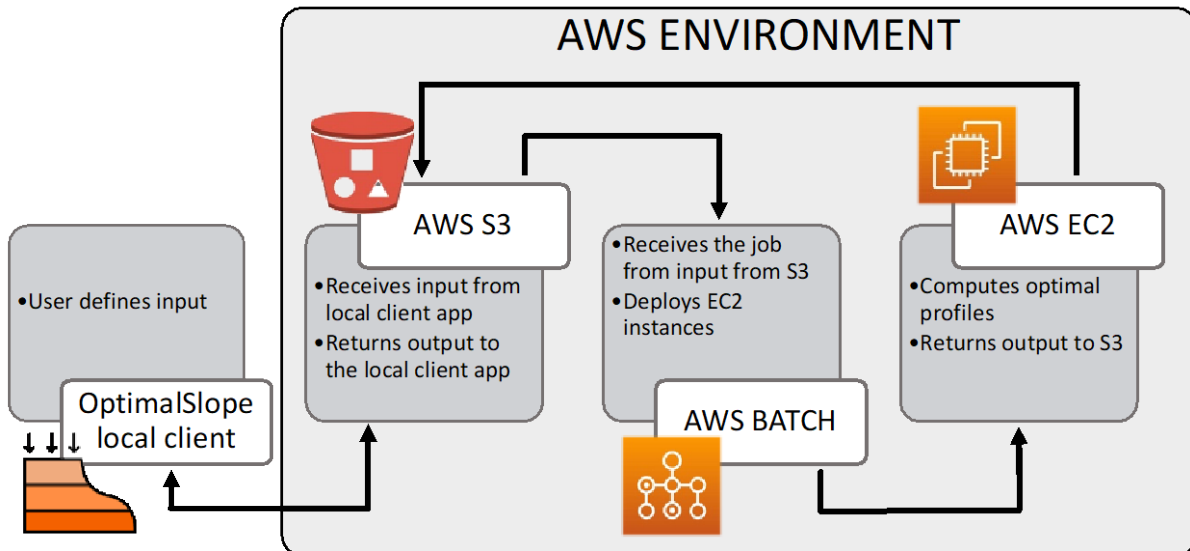


Figure 8 OptimalSlope AWS Environment.

6 Results

The OSAs for the cross sections described in Section 4 are reported in Figure 9. We sampled 21 different cross sections, each characterized by a different relationship between c , ϕ and dip of the failure surface. For each of them, the optimal profiles were calculated with OptimalSlope, while for the planar profiles, we used Rocscience Slide2.

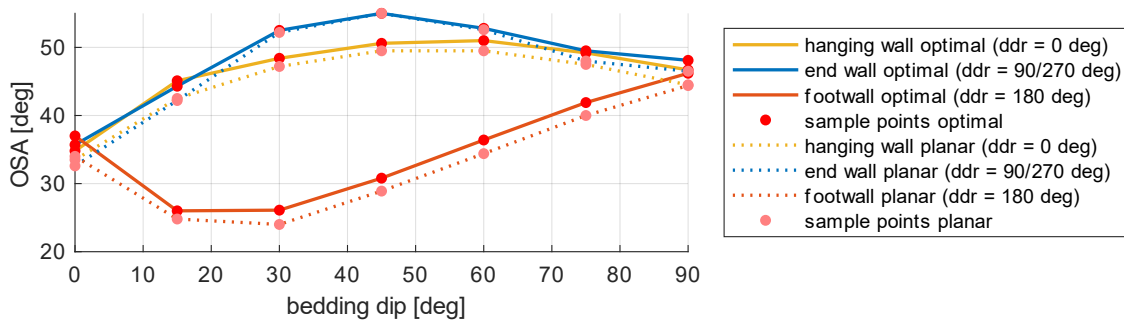


Figure 9 Bedding dip vs OSA of the optimal and planar pitwall profiles for different cross sections azimuth.

Figure 10 reports a graphical comparison, divided by cross section azimuth, between the OSA of the planar pitwall profiles and the optimal pitwall profiles. Overall, the optimal profile is steeper than the planar profile up to 3.1 degrees. However, for the pitwall profiles with bedding dip equal to 30, 45 and 60 degrees and cross section azimuth equal to 90/270 degrees, the improvement in OSA of the optimal profile over the planar one is almost negligible because the relationships between c , ϕ and (apparent) dip of the failure surface are almost equivalent to the one of the anisotropic rock mass (i.e. $c = 500$ kPa and $\phi = 31.5$ degrees constant for all values of dip of the failure surface). These relationships allow for an OSA almost equivalent to the maximum interramp angle. In particular, for the cross section with bedding dip 45 degrees and cross section azimuth 90

degrees, only a planar slope profile is obtained since the bench-face inclination and minimum berm width limit the maximum OSA of the pitwall to the value of the interamp angle, resulting in a FoS equal to the minimum acceptable value of 1.3. Subsequently, because the geometry of the benches entirely dictates the OSA of the profile, this profile cannot be improved by OptimalSlope, and the pitwall profiles adopted in this cross section for both types of design are the same.

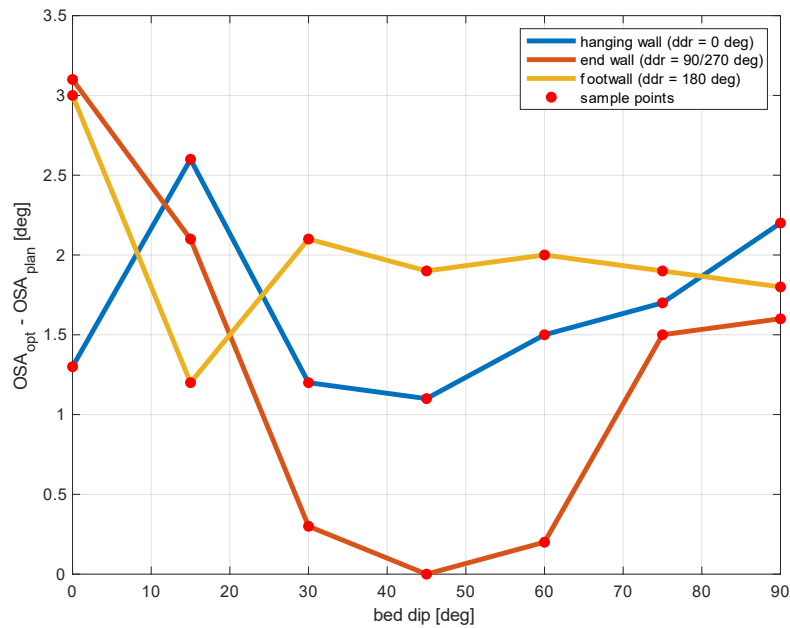


Figure 10 Bedding dip vs difference between OSA of the planar pitwall profile and the optimal pitwall profile for different cross sections azimuth.

As it emerges from Figure 10, the optimal profile is overall steeper than the planar profile up to 3.1 degrees. The pitwall profiles for the case of 75 degree bedding dip are plotted in Figure 11. The FoS of each pitwall profile was verified by a LEM analysis with the Morgenstern-Price method, which is a rigorous LEM method where all equations of equilibrium are imposed on all slices (Morgenstern & Price 1965), in Rocscience Slide2 using non-circular failure surface and other default settings including optimisation routines. A sensitivity analysis was conducted to check the independence of the results from the number of slices adopted, resulting in a final number of slices equal to 200.

The pitwall profiles employed in the LEM analyses are also reported in Figure 11 bottom row for the pit design adopting planar profiles, and top row for the pit design adopting optimal profiles together with their FoS, critical failure surface and line of trust. In all the cases, the FoS found is less than 1% from the target value of 1.30. In conclusion, the FoS values of the pitwall profiles found by OptimalSlope were independently verified by an industry-standard geotechnical software, confirming that the pitwall profiles determined by OptimalSlope are steeper whilst satisfying the same FoS value as their planar counterparts.

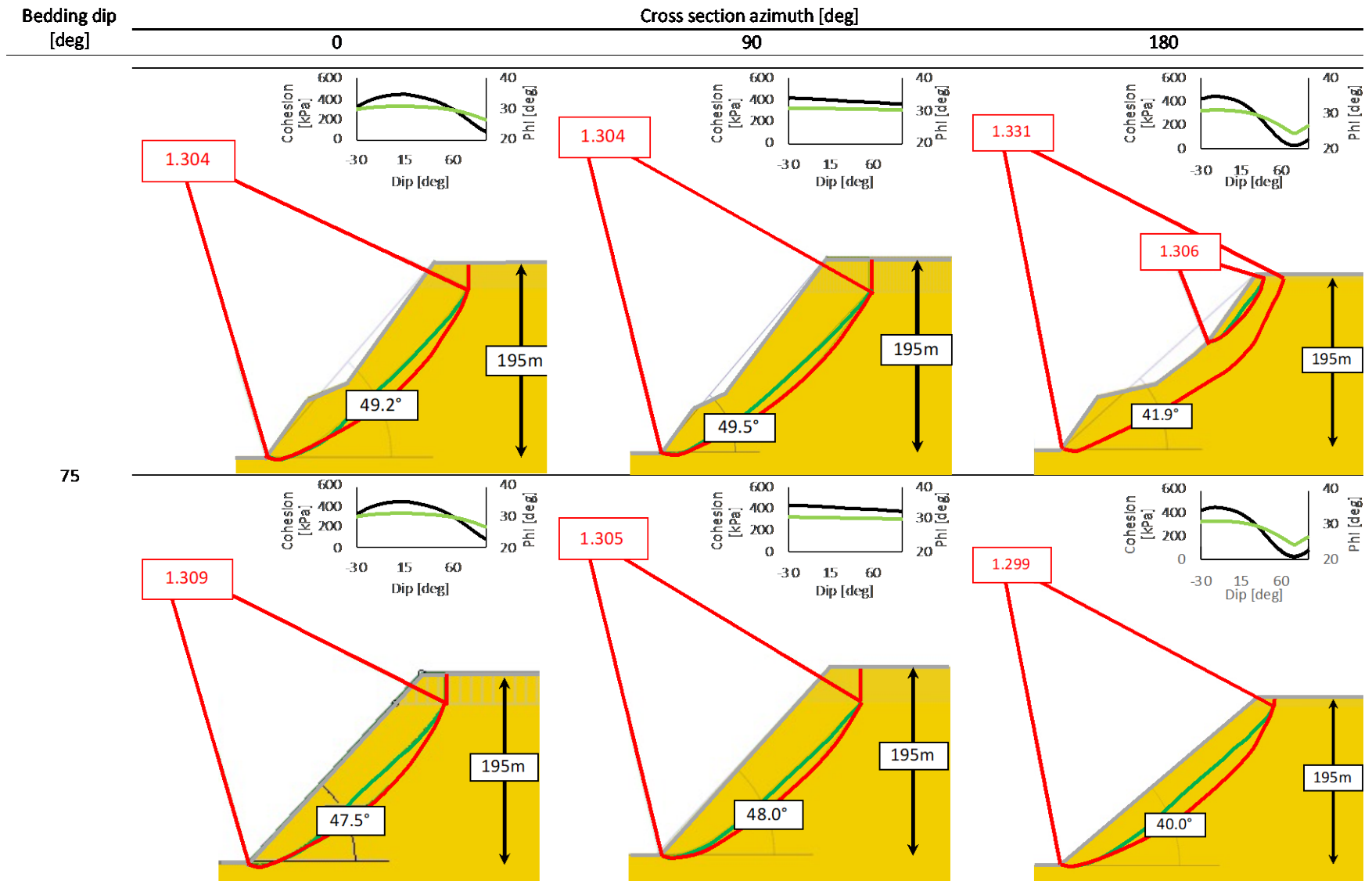


Figure 11 Bedding dip 75 degrees, top row optimal profiles, and bottom row planar profiles for different cross section azimuth. In red is the critical failure mechanism (local and global). In green is the line of trust. The graph on the top right of each figure shows the relationship between c , ϕ and the (apparent) dip of the failure surface.

7 Conclusions

A new methodology is presented to determine geotechnically optimal profiles, i.e. profiles that maximise the overall slope angle for a prescribed factor of safety, for anisotropic rock masses. The methodology presented is very general since shear strength anisotropy due to both intact rock and the presence of discontinuities such as beddings and joint sets is accounted for. To validate the methodology a discontinuity dataset for Cretaceous aged siltstone with 8 different joint sets and one main bedding from an existing open pit mine project was considered.

Optimal profiles were determined for three pitwall orientations: footwall, hanging wall and side walls. From the simulations performed with OptimalSlope emerges that optimal pitwall profiles can significantly increase the Overall Slope Angle in comparison with planar profiles featured by the same Factor of Safety up to 3 degrees. LEM stability analyses of all the profiles were also performed by Rocscience Slide 2 to independently verify the FoSs of the optimal profiles obtained.

The improvements reported in terms of pitwall inclinations, all above 1 degree apart from three cases, are significant and of similar magnitude as those reported in other mine case studies where OptimalSlope was applied to isotropic rock masses (Utili et al. 2022, Agosti et al. 2021a, b). In those case studies, the use of the optimal profiles determined by OptimalSlope as pitwall profiles led to Net Present Value improvements in the order of tens of USD millions together with important carbon footprint reductions achieved due to significant reduction of excavated waste rock.

References

- Agosti, A., Utili, S., Gregory, D., Lapworth, A., Samardzic, J., Prawasono, A. (2021). Design of an open-pit gold mine by optimal pitwall profiles. *CIM Journal* 12: 1–20. <https://doi.org/10.1080/19236026.2021.1979382>.
- Agosti, A., Utili, S., Valderrama, C., Albornoz, G. (2021). Optimal pitwall profiles to maximise the overall slope angle of open pit mines: the McLaughlin Mine. In Dight (ed.), *SSIM 2021: Second International Slope Stability in Mining, Australian Centre for Geomechanics, Perth*. pp. 69–82. https://doi.org/10.36487/ACG_repol2135_01.
- Amazon Web Services Inc. (2022) AWS Batch - User Guide.
- Call, RD. (1992). Slope Stability. In Hartman (ed.), *Mining Engineering Handbook 2nd ed. vol. 1*, Soc. for Mining, Metallurgy, and Exploration, Littleton.
- Chen, WF. (1975). *Limit analysis and soil plasticity*. Elsevier Scientific Pub. Co, New York.
- Colak, K., Unlu, T. (2004). Effect of transverse anisotropy on the Hoek–Brown strength parameter “mi” for intact rocks. *Int J Rock Mech Min Sci* 41: 1045–52.
- Cylwik, SD. (2022). “3D/2D Anisotropic Strength Estimation Worksheet”. Call & Nicholas, Inc., Accessed 13 June 2022, <https://www.cnitucson.com/publications.html>.
- Cylwik, SD. (2021). Three-Dimensional Anisotropic Shear Strength of Jointed Rock Masses. *55th US Rock Mechanics/Geomechanics Symposium of the American Rock Mechanics Association*, Houston.
- Darling, P. (2011) *Mining engineering handbook*. 3rd ed. Society for Mining, Metallurgy, and Exploration, Englewood.
- Hartman, HL. (1992). *Mining engineering handbook*. 2nd ed. Society for Mining, Metallurgy, and Exploration, Littleton.
- Hoek, E., Bray, J. (1977). *Rock Slope Engineering*. The Institution of Mining and Metallurgy, London.
- Hoek, E., Brown, ET. (1980). Empirical Strength Criterion For Rock Masses. *Journal Of The Geotechnical Engineering Division* 106: 1013-1035.
- Hoek, E., Carranza-Torres, C., Corkum, B. (2002). Hoek-Brown failure criterion – 2002 edition. *Proc NARMS-TAC Conference, Toronto* pp. 267–73.
- Hustrulid, W., Kuchta, M., Martin, R. (2013). *Open pit mine planning & design*. CRC Press, London.
- Ismael, MA., Imam, HF., El-Shayeb, Y. (2014) .A simplified approach to directly consider intact rock anisotropy in Hoek–Brown failure criterion. *Journal of Rock Mechanics and Geotechnical Engineering* 6: 486–92.
- Jeldes, IA., Drumm, EC., Yoder, DC. (2015). Design of Stable Concave Slopes for Reduced Sediment Delivery. *J Geotech Geoenviron Eng* 141: 04014093.
- Lo, KY. (1965). Stability of slopes in anisotropic soils. *Soil Mechanics Foundation Division ASCE* 91: 85-106.
- Martin, D., Stacey, P. (2018). *Guidelines for open pit slope design in weak rocks*. CSIRO Publishing, Clayton, Australia.

Mercer, K.G. (2012). The history and development of the anisotropic linear model: Part 1. *Australian Centre for Geomechanics, July 2012 Newspaper* .

Morgenstern, N., Price, V.E. (1965). The analysis of the stability of general slip surfaces. *Geotechnique* 15: 79-93.

Newman, J. (1890). *Earthwork slips and subsidences upon public works*. E. & F. N. Spon, London.

Nicholas, D.E., Sims, D.B. (2000). Collecting and Using Geologic Structure Data for Slope Design. In Hustrulid (ed.) *Slope Stability in Surface Mining*, Society of Mining, Metallurgy, and Exploration, Inc: Littleton.

Randolph, M. (2011) Current trends in mining. In Darling (ed.), *Mining engineering handbook*. 3rd ed. Society for Mining, Metallurgy, and Exploration, Englewood, pp. 11–21.

Read, J., Stacey, P. (2009). *Guidelines for open pit slope design*. CSIRO Pub., Collingwood.

Ryan, T.M., Pryor, P.R. (2001). Designing Catch Benches and Interramp Slopes. In Hustrulid, McCarter, Van Zyl (eds.), *Slope Stability in surface mining*. Society for Mining, Metallurgy, and Exploration, pp. 27–38.

Ryan, T.M. (2005). Shear Strength of Closely Jointed Porphyry Rock Masses. *40th US Rock Mechanics/Geomechanics Symposium American Rock Mechanics Association*.

Saroglu, H., Tsiambaos, G. (2007) A modified Hoek-Brown failure criterion for anisotropic intact rock. *Int J Rock Mech & Min Sci* 45: 223–34.

Stockton, E., Leshchinsky, B.A., Olsen, M.J., Evans, T.M. (2019). Influence of both anisotropic friction and cohesion on the formation of tension cracks and stability of slopes. *Engineering Geology* 249: 31–44.

Taylor, D.W. (1937). Stability of earth slopes. *Journal of the Boston Soc of Civil Engineers* 24: 197–247.

Utili, S., Agosti, A., Morales, N., Valderrama, C., Pell, R., Albornoz, G. (2022). Optimal Pitwall Shapes to Increase Financial Return and Decrease Carbon Footprint of Open Pit Mines. *Mining, Metallurgy & Exploration* 39: 335–355 <https://doi.org/10.1007/s42461-022-00546-8>.

Utili, S., Nova, R. (2007). On the optimal profile of a slope. *Soils and Foundations* 47: 717–29.

Utili, S. (2013). Investigation by limit analysis on the stability of slopes with cracks. *Géotechnique* 63: 140–54.

Utili, S. (2016). OptimalSlope: Software for the determination of optimal profiles for slopes and pitwalls. OptimalSlope Ltd..

Vahedifard, F., Shahrokhbabadi, S., Leshchinsky, D. (2016). Optimal profile for concave slopes under static and seismic conditions. *Canadian Geotechnical Journal* 53: 1522–32.

Vo, T., Russell, A.R. (2017). Stability charts for curvilinear slopes in unsaturated soils. *Soils and Foundations* 57: 543–56.